Traces of Vortices in Superfluid Helium Droplets

Luis F. Gomez, Evgeny Loginov, and Andrey F. Vilesov

Phys. Rev. Lett. **108**, 155302 — Published 10 April 2012

DOI: 10.1103/PhysRevLett.108.155302

Traces of Vortices in Superfluid Helium Droplets

Luis F. Gomez, Evgeny Loginov[1], and Andrey F. Vilesov

Department of Chemistry, University of Southern California, Los Angeles, CA 90089

1. Present address: SICPA SA, CH-1008 Prilly, Switzerland

02-23-2012

Abstract

We report on the observation of vortices in superfluid ^{4}He droplets produced in the expansion of liquid He. The vortices were traced by introducing Ag atoms into the droplets, which clustered along the vortex lines. The Ag clusters were subsequently surface-deposited and imaged via electron microscopy. The prevalence of elongated track-shaped deposits shows that vortices are present in droplets larger than about 300 nm and that their lifetime exceeds a few milliseconds. We discuss the possible formation mechanisms and the stability of the vortices.

First observed in ^{4}He, quantum vortices are one of the most dramatic hallmarks of superfluidity. [1-3] In contrast to a normal fluid, which will rotate as a solid body when its container moves at low angular velocity, a superfluid will remain at rest. However, above a certain critical angular velocity the thermodynamically stable state of a superfluid includes one or more quantum vortices. Such a vortex can be characterized by a macroscopic wave function and quantized velocity circulation in units of $\kappa = \frac{h}{M}$, where h is Planck's constant and M is the mass of the ^{4}He atom. [2-3] Recently, the study of vorticity was extended to finite systems such as Bose-Einstein condensates (BECs) confined to traps. [3-4] The transfer of energy and angular momentum in finite systems between quantized vortices and surface excitations is of particular interest as it defines the nucleation dynamics, shape, and stability of the involved vortices. [3-4] In comparison to confined BECs, ^{4}He droplets are self-contained and present a case for the strongly interacting superfluid. Moreover, the diameter of a vortex core which is approximately 0.2 nm in superfluid He [2] is small relative to the droplet size, suggesting a three dimensionality of the vortices in droplets. Vorticity in He droplets has therefore attracted considerable interest. [5-8]

Early attempts at observing vortices in mm-sized He droplets include experiments with magnetic levitation. [9] A critical angular velocity necessary for the formation of vortices in droplets has been estimated. [10] Calculations predict that vortices in superfluid He droplets are curved in shape and that there exists a substantial barrier in free energy to their formation. [11] It was also shown that curved vortices must be stable in nanometer-sized droplets because of their smaller energy per angular momentum relative to evaporation or the possible accepting modes of the droplet such as surface ripplons. [6] According to calculations [7, 12], the vortices can be stabilized in droplets consisting of just a few hundred He atoms by pinning foreign particles to the vortex lines. The trapping of electrons and ions was instrumental in early observations of vortex rings in bulk liquid He. [13] Therefore, the possibility of trapping probe atoms and molecules along vortices in He droplets was considered [5, 14]. However, thus far all spectroscopic observations in He droplets can be explained without invoking vorticity. [5-8]

Vortices in bulk superfluid He, as well as in BECs, are often produced by the application of a rotating perturbation [2-4]. Such an approach is difficult to apply to the droplets in a fast-moving beam; the droplets themselves must carry sufficient energy and angular momentum for a vortex to exist. It was therefore concluded that vortices are not produced efficiently in a typical beam experiment involving the capture of impurities or

during the growth of the droplets from a gas expansion. [6] In this work, we circumvented these limitations by producing He droplets containing vortices via fragmentation of a cryogenic He fluid. [15] The vortices were traced by introducing Ag atoms into the droplets, which clustered along the vortex lines as previously demonstrated in bulk liquid He using H_2 and Au clusters (see [16-17] and references therein).

Experiments in beams of He droplets have been reviewed previously. [8, 18-19] A schematic of the experiment is shown in Fig. 1. Helium droplets are produced by expansion of He, at 20 bar and a temperature T_0 = 5.4 – 7 K, into vacuum through a nozzle of diameter D = 5 μm. The droplets cool rapidly via evaporation and reach a temperature of 0.37 K [20], which is well below the superfluid transition temperature T_λ = 2.17 K [2-3]. Further downstream the droplets capture 10^3 – 10^6 Ag atoms in an oven. [21] The droplets are then collided against a thin carbon film substrate at room temperature. [21] Upon impact, the droplets evaporate leaving the Ag traces on the surface, which are subsequently imaged via a transmission electron microscope (TEM). More details are provided in the Supplementary Online Material. [22]

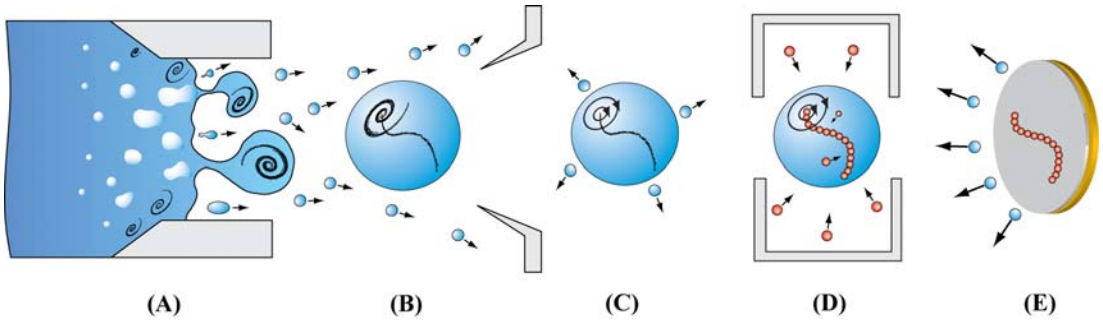

Fig. 1. Schematic of the experiment. (A) He fluid expands in vacuum and (B) breaks up into rotating droplets. (C) A quantum vortex is formed following evaporative cooling of the droplet to below T_λ. (D) The droplet is doped with Ag atoms, which are attracted to the vortex core. (E) The droplet then collides with the carbon surface leaving behind the Ag trace whereas the He evaporates.

Figure 2, A – C shows some typical TEM micrographs of the Ag aggregates (black traces) grown in He droplets with average diameters of 100, 300, and 1000 nm, respectively. [15] The micrographs reveal that the shapes of the obtained Ag traces change remarkably with increased He droplet size. The aggregates obtained in the smallest droplets are round in shape (Fig. 2A), whereas those obtained in the larger droplets are track-like (Fig. 2, B and C). The number of tracks observed in the micrographs is in agreement with the measured flux of the He droplets [15]. Moreover, the tracks in Fig. 2, B and C are well-separated by empty regions in the micrographs. Therefore, we conclude that each track results from the impact of a single, doped He droplet. As control experiments, the samples were exposed to an effusive beam of Ag atoms emanating from the oven, in the absence of He droplets, which was kept at the same temperature as in Fig. 2C. At a deposition time of 2 s, as in Fig. 2C, no deposits could be detected in the TEM images. At a much longer exposure time of 30 min a high density of evenly distributed round clusters smaller than about 2 nm in diameter was observed. Therefore we conclude that diffusion of Ag atoms and clusters on the substrate surface cannot cause the observed elongated tracks.

Some representative tracks are shown at higher magnification in Fig. 3. Each of the tracks consists of tens of segments having a cross section of about 10 nm, as shown in the inset to Fig. 3B. Analysis of about 100 images such as in Fig. 3 A, B gives the length of the tracks to be (540 ± 220) nm, which is comparable to the average diameter of the droplets of about 700 nm after being doped by Ag. [22] The scatter is consistent with the mean square deviation of the droplet diameter of approximately 35% [22] and with the multitude of track shapes. The number of Ag atoms in a track of this average length was estimated assuming a bulk density and a cylindrical track shape to be about 10^6 in agreement with the number of captured Ag atoms. [22]

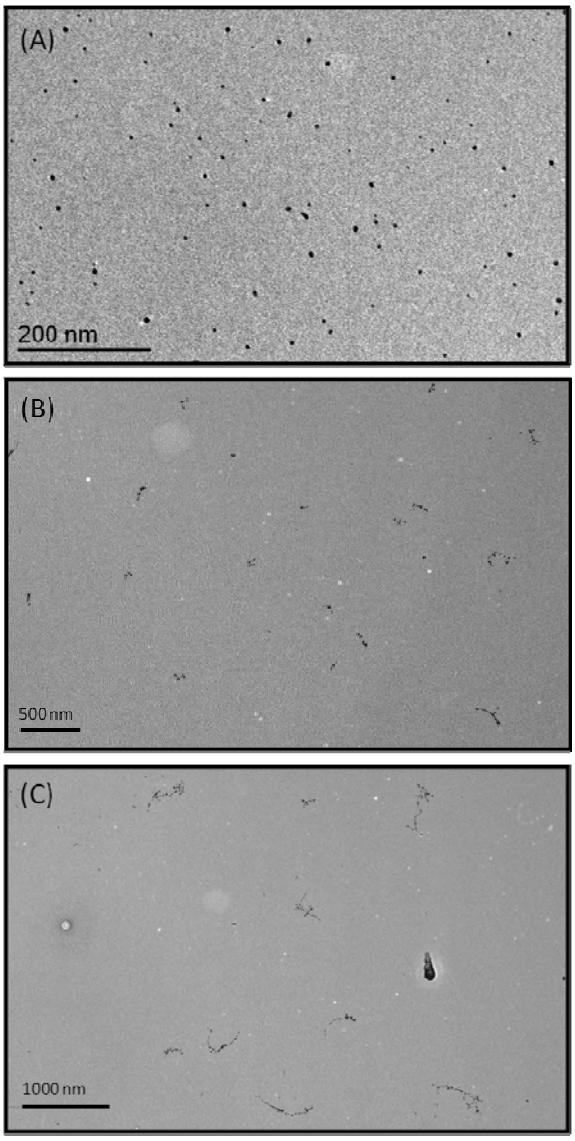

Fig. 2. TEM micrographs obtained upon deposition of Ag-doped droplets of average diameter (A) 100 nm, (B) 300 nm, and (C) 1000 nm and average number of He atoms $\langle N_{He} \rangle = 10^7$, 3×10^8, and 1.7×10^{10}, respectively. The droplets were attained at a nozzle temperature $T_0 = 7$, 6 and 5.4 K, respectively. [15] Exposure times to the droplet beam are 120 sec, 4 sec, and 2 sec, respectively. Large dark spot on right side of (C) is artifact likely introduced during sample transfer to the TEM.

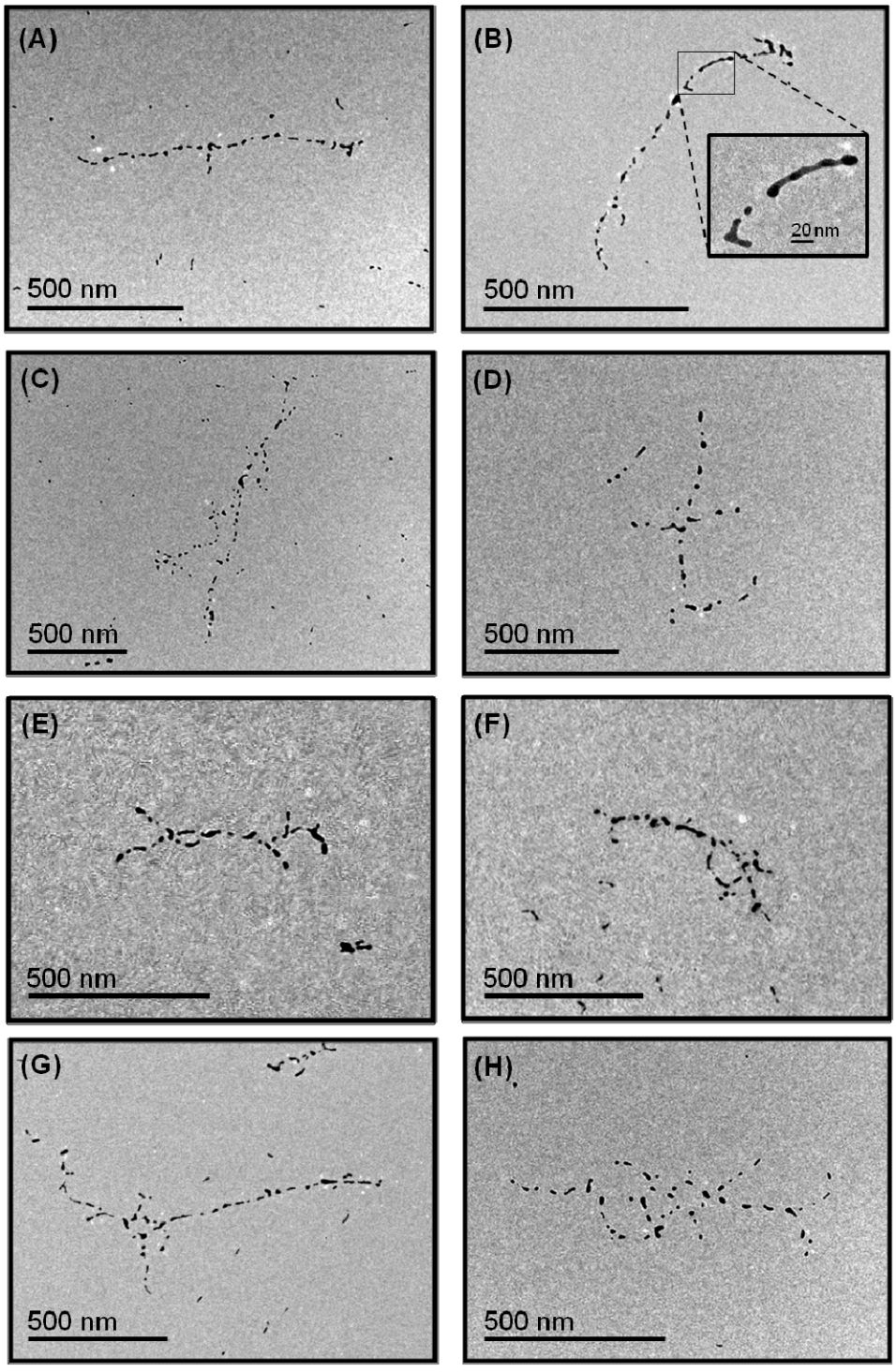

Fig. 3. Typical Ag traces obtained in 1000 nm He droplets. The inset to panel (B) shows an enlarged track segment.

In an isotropic droplet, the recombination of Ag atoms will likely result in fractal aggregates [23], as are often encountered in colloidal chemistry. In order for the aggregates to assume track shapes of length comparable to droplet diameter a long-range guiding force, such as the force of attraction of foreign particles to the core of a vortex line in a superfluid [7], is required. An impurity particle does not partake in the circulation of the superfluid, so trapping of a particle in the vortex core leads to a reduction in the kinetic energy of the superfluid by about 5 K, as calculated for Xe atoms. [12] The binding of Ag atoms and small Ag clusters formed inside the He droplets [24] to the vortex core and subsequent aggregation of the trapped particles leads to the formation of the observed elongated aggregates. A similar mechanism has been well-documented in bulk superfluid He [16-17]. Therefore, we conclude that aggregation in vortices provides the most likely explanation of the observed elongated aggregates. In contrast, the formation of much shorter, linear molecular clusters such as $(HCN)_7$ in small He droplets of less than 10 nm diameter ($N_{He} < 10^4$) has been attributed to the strong dipole-dipole interaction of the HCN molecules. [25] This mechanism, however, is not applicable to the atoms and metal clusters used in this work which are devoid of a permanent dipole moment. Furthermore, van der Waals interactions between the recombining particles are short range (of the order of three diameters for spherical particles) [26] and strongest for aggregates with large surface contact (such as the T-shaped configuration of three particles), so they are not expected to facilitate the formation of long tracks.

The prevalence of the track-shaped deposits indicates that vortices are present in droplets larger than about 300 nm and that they survive the 1.5 ms flight time from nozzle to Ag oven. The appearance of the vortices in the large droplets correlates with the different regimes of the nozzle beam expansion. Our recent work [15] indicates that droplet formation occurs within the nozzle for $T_0 < 6.5$ K (as in Fig. 2, B and C). At $T_0 = 7$ K (Fig. 2 A), the fluid breaks up into droplets beyond the nozzle which may not be favorable for the formation of vortices.

The density of Ag is approximately a factor of 80 larger than that of liquid He and its binding energy is 5000 times larger; it is therefore likely that during the impact of the doped He droplet the Ag inclusions move nearly ballistically toward the surface whereas the He evaporates. In this way, the TEM images (Fig. 3) represent two-dimensional projections of the vortex traces as they exist in the He droplets. The most common deposit shape, with an occurrence of about 40%, is tracked and curved (Fig 3, A – B) which must result from single curved vortices, as predicted theoretically. [11] In many instances the tracks have short (Fig.

3, A – B) or longer branches (Fig. 3, C – D). Such longer branches may indicate the presence of multiple vortices within the same droplet. Fig. 3E resembles the projection of two braided traces which is consistent with two gyrating parallel vortices. A small number of traces have loops (Fig. 3, F and G) which may indicate the presence of both vortex lines and vortex rings in the same droplet. Finally, Fig. 3H resembles a tangle of vortices.

The state of the He fluid during the expansion is defined by its isentropes. Accordingly, an expansion starting at $T_0 = 5.4$ K, $P_0 = 20$ bar, as in Fig. 2C and in Fig. 3, will reach the phase separation line inside the nozzle where the fluid will break up into droplets at $T \approx 4.1$ K, $P \approx 0.9$ bar. [15, 27] Thus, the droplets are initially composed of normal fluid. The temperature of the droplets at a distance S from the nozzle of diameter D can be estimated from the He saturated vapor density [28] and the local number density, n, of the He gas which follows $n \approx n_0 \frac{D^2}{S^2}$. Here, n_0 is the number density of the He gas at phase separation. According to our estimate, the temperature of the droplets approaches T_λ at $S =$ 0.02 mm after 10^{-7} s of expansion assuming a droplet velocity $v_D = 173$ m/s [15]. At $S = 0.2$ mm and after 10^{-6} s, the temperature falls to ≈1 K corresponding to a superfluid with a normal fluid fraction of only about 7×10^{-3} [28]. Subsequently, the droplets cool even further by evaporation to 0.37 K. [20]

The spontaneous formation of vortices during the rapid superfluid transition in bulk liquid He has caught the attention of many as a model of the creation of cosmic strings during the early expansion of the Universe. [29] In this work, however, the rotating droplets may originate from asymmetries in the flow through the nozzle channel. Once the droplet becomes superfluid, solid body rotation is no longer feasible and the rotation takes the form of a vortex. [6] [11] Estimates show that a normal fluid droplet of 1000 nm diameter rotating at an equatorial velocity of about 0.2 m/s has sufficient rotational energy and angular momentum for the creation of a rectilinear vortex. Such a rotational velocity is feasible for a droplet moving at $v_D \approx 173$ m/s through a narrow $D = 5$ μm diameter nozzle. In addition, the corresponding angular velocity of about 4×10^5 rad/s would remain well below the stability limit of the droplet at about 10^7 rad/s. [30]

Our expansion is characterized by a Reynolds number $R_e = \frac{v_D \cdot D}{\nu} \approx 4\times10^4$, which is higher than the typical threshold for turbulence at about 3×10^3. Here $\nu \approx 2.5\times10^{-8}$ m^2/s is the kinematic viscosity of normal fluid He [28]. Therefore, the interaction of the fast moving He fluid with the walls of the nozzle can generate classical vortices [31] which become trapped

in the droplets upon fragmentation. In a normal fluid, a vortex has a solid body rotating core of diameter d which will increase with time, τ, according to $\tau = \frac{d^2}{16\nu}$. [32] Therefore the lifetimes of vortices in normal fluid droplets of diameter 100 and 1000 nm are estimated at $\tau \approx 2.5\times10^{-8}$ and 2.5×10^{-6} s, respectively. It follows that, although the lifetime of classical vortices in the smaller droplets is too short, vortices will persist in the larger droplets at T_λ and can contribute to quantum vortex formation.

If the angular momentum of a superfluid droplet, L_D, is equal to $\hbar \cdot N_{He}$ then a single rectilinear vortex is formed; a smaller value of L_D corresponds to the formation of a curved vortex [6]. If the droplet possesses a larger angular momentum, however, the resulting quantum vortex will be formed in a non-stationary state and will eventually decay into a collection of unit circulation vortices of different shapes and orientation. Some of the branched vortices as well as the other intriguing shapes shown in Fig. 3 may indeed originate from the evolution of such non-stationary states during the time-of-flight of the droplets.

Also interesting, our results allow for an estimation of the mean square vorticity, ω, in the expansion according to $\omega = \kappa \cdot L$ [31] where L is the length of quantum vortex lines per unit volume. Assuming that each of the 300 nm diameter droplets contains a single vortex spanning the droplet diameter one obtains $\omega \approx 10^6$ s^{-1}. This is a factor of approximately 10^3 larger than typically observed in turbulent bulk superfluid He. [31]

We comment now on the possible origins of the segmentation of the Ag traces. It was shown that 10 μm H_2 clusters attached to vortices in bulk superfluid He are uniformly spaced along the vortex core [16] and hypothesized that clusters attached to a vortex repel each other through a mechanism which remains to be understood. In contrast, the deposits obtained in this work often contain intact, elongated Ag segments (Fig. 3, A – B) indicating that the traces may actually be continuous inside the droplets. From the droplet velocity, the kinetic energy of the surface impact is estimated at about 0.02 eV per Ag atom, which is much less than the binding energy of Ag atoms in solid of about 3 eV. Therefore, the aggregates should remain largely intact although the impact may fracture the traces into segments. Any subsequent reconstruction is expected to be more pronounced in smaller Ag clusters and may affect our ability to detect vortices in the small 100 nm diameter droplets. In the future, measurements should be expanded to imaging by means of X-ray diffraction inside the droplets in order to attain the structure of the traces as well as to assess the smallest size droplet which can carry a vortex.

Very recently, the formation of bundles of metallic nano-filaments upon the ablation of metals in bulk liquid He by a focused pulsed laser beam was reported. [17] The observation of similar nano-filaments in both superfluid and normal He indicates that their formation occurs on a short time scale close to the hot environment of the ablation spot, by trapping and coalescence of the particles in turbulent eddies in the ablation area. [17] Subsequently, the nano-filaments and small spherical particles aggregate into cm-long bundles along the vortex lines in superfluid He, whereas in the normal fluid He the fragments are spread uniformly. The very different experimental conditions of Ref. [17] and this work render the results difficult to compare. In this work, the Ag atoms enter the droplets which remain at $T < T_\lambda$ throughout. On the other hand, the violent ablation process in Ref. [17] provides for poorly characterized initial conditions. In this respect, the levitation of superfluid droplets in high vacuum [9] followed by their controllable doping with atoms may provide an ideal system for studying vortex-guided aggregation in macroscopic samples of superfluid He.

In conclusion, our results indicate that superfluid He droplets of diameters larger than 300 nm, produced upon fragmentation of a free fluid-jet, contain single and multiple vortices. The vortices may originate from the solid body rotation of the normal fluid droplets or from classical vortices in the expanding fluid that are entrapped by the droplets upon fragmentation. After entering vacuum, the droplets cool down and become superfluid within less than 1 μs where classical vortices and rotations may give rise to quantum vortices. In addition, we have observed some rather unusual deposit shapes that indicate the formation during the rapid superfluid transition of non-stationary vortex states.

The authors are grateful to J. P. Toennies and V.V. Kresin for their careful reading of the manuscript and valuable discussions. This work was supported by NSF grant CHE-1112391.

References

1. R. P. Feynman, in *Progress in low temperature physics*, edited by C. J. Gorter (North-Holland Publishing Company, Amsterdam, 1955), Vol. 1, pp. 1.
2. R. J. Donnelly, *Quantized Vortices in Helium II*. (Cambridge University Press, Cambridge, 1991).
3. L. Pitaevskii, and S. Stringari, *Bose-Einstein Condensation*. (Clarendon Press, Oxford, 2003).
4. A. L. Fetter, Rev. Mod. Phys. **81**, 647 (2009).
5. J. D. Close, F. Federmann, K. Hoffmann, and N. Quaas, J. Low Temp. Phys. **111**, 661 (1998).
6. K. K. Lehmann, and R. Schmied, Phys. Rev. B **68**, 224520 (2003).
7. M. Barranco, R. Guardiola, E. S. Hernandez, R. Mayol, and M. Pi, J. Low Temp. Phys. **142**, 1 (2006).
8. F. Stienkemeier, and K. K. Lehmann, J. Phys. B **39**, R127 (2006).
9. M. A. Weilert, D. L. Whitaker, H. J. Maris, and G. M. Seidel, J. Low Temp. Phys. **106**, 101 (1997).
10. L. Pitaevskii, and S. Stringari, Z. Phys. D **16**, 299 (1990).
11. G. H. Bauer, R. J. Donnelly, and W. F. Vinen, J. Low Temp. Phys. **98**, 47 (1995).
12. F. Dalfovo, R. Mayol, M. Pi, and M. Barranco, Phys. Rev. Lett. **85**, 1028 (2000).
13. G. W. Rayfield, and F. Reif, Phys. Rev. **136**, A1194 (1964).
14. F. Ancilotto, M. Barranco, and M. Pi, Phys. Rev. Lett. **91**, 105301 (2003).
15. L. Gomez, E. Loginov, R. Sliter, and A. F. Vilesov, J. Chem. Phys. **135**, 154201 (2011).
16. M. S. Paoletti, R. B. Fiorito, K. R. Sreenivasan, and D. P. Lathrop, J. Phys. Soc. Jpn. **77**, 111007 (2008).
17. V. Lebedev, P. Moroshkin, B. Grobety, E. Gordon, and A. Weis, J. Low Temp. Phys. **165**, 166 (2011).
18. C. Callegari, K. K. Lehmann, R. Schmied, and G. Scoles, J. Chem. Phys. **115**, 10090 (2001).
19. J. P. Toennies, and A. F. Vilesov, Angew. Chem. Int. Ed. **43**, 2622 (2004).
20. M. Hartmann, R. E. Miller, J. P. Toennies, and A. Vilesov, Phys. Rev. Lett. **75**, 1566 (1995).
21. E. Loginov, L. F. Gomez, and A. F. Vilesov, J. Phys. Chem. A **115**, 7199 (2011).
22. See supplementary material at ..... for more experimental details.
23. S. G. Alves, A. F. Vilesov, and S. C. Ferreira, J. Chem. Phys. **130**, 244506 (2009).
24. E. Loginov, L. F. Gomez, N. Chiang, A. Halder, N. Guggemos, V. V. Kresin, and A. F. Vilesov, Phys. Rev. Lett. **106**, 233401 (2011).
25. K. Nauta, and R. E. Miller, Science **283**, 1895 (1999).
26. J. N. Israelachvili, *Intermolecular and surface forces*, 3 ed. (Academic Press, San Diego, Oxford, Amsterdam, 2011).
27. H. Buchenau, E. L. Knuth, J. Northby, J. P. Toennies, and C. Winkler, J. Chem. Phys. **92**, 6875 (1990).
28. R. J. Donnelly, and C. F. Barenghi, J. Phys. Chem. Ref. Data **27**, 1217 (1998).
29. W. H. Zurek, Nature **317**, 505 (1985).
30. R. A. Brown, and L. E. Scriven, Proc. R. Soc. A **371**, 331 (1980).
31. R. J. Donnelly, in *Quantized vortex dynamics and superfluid turbulence*, edited by C. F. Barenghi, R. J. Donnelly and W. F. Vinen (Springer, Berlin, 2001), pp. 17.
32. J.-Z. Wu, H.-Y. Ma, and M.-D. Zhou, *Vorticity and Vortex Dynamics*. (Springer, Berlin, Heidelberg, 2006).